Supplemental Information

Rational compatibility in ternary matrix enables all-small-molecule organic solar cells with over 16% efficiency

Mengyun Jiang,[a] Hairui Bai,[a] Hongfu Zhi,[a] Lu Yan,[a] Han Young Woo,[b] Lijia Tong,[c] Jinliang Wang,[a*] Fujun Zhang[d*] and Qiaoshi An[a*]

[a] Key Laboratory of Cluster Science of Ministry of Education, Beijing Key Laboratory of Photoelectronic/Electrophotonic Conversion Materials, School of Chemistry and Chemical Engineering, Beijing Institute of Technology, 100081, Beijing, China.

[b] Department of Chemistry, Korea University, Seoul 136-713, Republic of Korea.

[c] Department of Basic Sciences, Air Force Engineering University, 710038, Xi'an, China.

[d] School of Science, Beijing Jiaotong University, 100044, Beijing, China.

*Correspondence: jinlwang@bit.edu.cn, fjzhang@bjtu.edu.cn and qsan@bit.edu.cn

1. Detailed experimental section

Materials

The small molecules B1 (Lot# NK526B), BO-4Cl (Lot# NK610A) and Y7 (Lot# KJ822B) were purchased from Solarmer Materials Inc and used as received**.** PNDIT-F3N (Lot# ETL23) was purchased from eFlexPV co. Ltd and PEDOT:PSS (clevios P VP Al 4083) was purchased from H.C. Starck co. Ltd.

ASM-OSCs fabrication and measurement

The patterned indium tin oxide (ITO) glass coated substrates (sheet resistance 15 Ω/□) were consecutively cleaned in ultrasonic baths containing detergent, de-ionized water and ethanol, respectively. Then, poly-(3,4-ethylenedioxythiophene):poly-(styrenesulphonicacid) (PEDOT:PSS) thin films were fabricated on the cleaned ITO substrates by spin-coating method at 5000 round per minute (RPM) for 40 s, and then annealed at 150 °C for 10 minutes in ambient conditions. After annealing treatment, the ITO substrates coated PEDOT:PSS films were transferred to a high-purity nitrogen-filled glove box to fabricate active layers. The small molecules B1, BO-4Cl and Y7 were dissolved in chloroform (CF) to prepare 20 mg ml^{-1} blend solutions. The contents of Y7 in acceptors (Y7 and BO-4Cl) are 0 wt%, 5 wt%, 10 wt%, 15 wt%, 20 wt%, 30 wt%, 50 wt%, 100 wt%, and the weight ratio of donor to acceptor is kept constant as 1:1. The blend solutions were spin-coated on PEDOT:PSS films in a high purity nitrogen-filled glove box to fabricate the active layers. The active layers were solvent vapor annealed with chlorobenzene in a 60 mm diameter dish for 80 s. The optimized thickness of the active layer is ~100 nm, which was measured by KLA-Tencor Alpha-Step D-600 Stylus Profiler. After that, PNDIT-F3N solution (0.5 mg ml^{-1} in methanol with 0.5 vol% acetic acid) was spin-coated on the top of active layers at 2000 RPM for 30 s. The cathode of Ag was deposited by thermal evaporation with a shadow mask under 10^{-4} Pa and the thickness of 100 nm was monitored by a quartz crystal microbalance. The active area of all-small-molecule organic solar cells (ASM-OSCs) is about 4 mm^2, which is defined by the overlap of ITO anode and Ag cathode.

Characterizations on films and ASM-OSCs

The ultraviolet-visible (UV-Vis) absorption spectra of pure B1, BO-4Cl and Y7 films were obtained using a Shimadzu UV-3101 PC spectrometer. The current density-voltage (*J-V*) curves of ASM-OSCs were measured in a high-purity nitrogen-filled glove box using a Keithley B2901A source meter. AM 1.5G irradiation at 100 mW cm^{-2} is provided by a simulator (SS-F5-3A, Enlitech, AAA grade, 70×70 mm^2 photobeam size) in glove box, which was calibrated by standard silicon solar cells (purchased from Enlitech). The external quantum efficiency (EQE) and internal quantum efficiency (IQE) spectra of ASM-OSCs were measured in air conditions by a solar cell spectral response measurement system (QE-R3011, Enlitech).

TPC, TPV and Photo-CELIV

Transient photovoltage (TPV), transient photocurrent (TPC) and photo-induce charge extraction linear increasing voltage (Photo-CELIV) were conducted with the Paioscarrier measurement system (FLUXiM AG, Switzerland). A high-power white LED is utilized as light source for TPV, TPC and photo-CELIV measurements. The integrated power of the LED is 72 mW cm^{-2}, and the spectrum distribution is mainly in the wavelength range of 440–470 nm and 540–630 nm, and the peak value located at 460 nm and 550 nm.

Charge mobility measurement by SCLC method

The structure of electron-only devices is ITO/ZnO/active layer/PDIN/Al and the structure of hole-only devices is ITO/PEDOT:PSS/active layer/MoO_3/Ag. The fabrication conditions of the active layer films are same with those for the OSCs. The charge mobilities are generally described by the Mott-Gurney equation[1-3]:

$$J = \frac{9}{8}\varepsilon_r\varepsilon_0\mu\frac{V^2}{L^3} \tag{1}$$

where J is the current density, ε_0 is the permittivity of free space (8.85×10^{-14} F/cm), ε_r is the dielectric constant of used materials, μ is the charge mobility, V is the applied voltage and L is the active layer thickness. The ε_r parameter is assumed to be 3, which is a typical value for organic materials. In organic materials, charge mobility is usually field dependent and can be described by the disorder formalism, typically varying with electric field, E=V/L, according to the equation[4-6]:

$$\mu = \mu_0 \exp[0.89\gamma\sqrt{\frac{V}{L}}] \tag{2}$$

where μ_0 is the charge mobility at zero electric field and γ is a constant. Then, the Mott-Gurney equation can be described by:

$$J = \frac{9}{8}\varepsilon_r\varepsilon_0\mu_0\frac{V^2}{L^3}\exp[0.89\gamma\sqrt{\frac{V}{L}}] \tag{3}$$

In this case, the charge mobilities were estimated using the following equation:

$$\ln(\frac{JL^3}{V^2}) = 0.89\gamma\sqrt{\frac{V}{L}} + \ln(\frac{9}{8}\varepsilon_r\varepsilon_0\mu_0) \tag{4}$$

AFM, TEM and GIWAXS

The surface morphology of the active layers was investigated by an optical microscope (OM) and atomic force microscopy (AFM) using a Dimension Icon AFM (Bruker) in a tapping mode. transmission electron microscopy (TEM) images of the active layers were obtained by using a JEOL JEM-1400 transmission electron microscope operated at 80 kV. The samples for AFM and TEM characterization were prepared under the same conditions compared with the active layers of the ASM-OSCs. The samples for TEM measurement were prepared by dissolving the PEDOT:PSS layer using deionized water and picked up the active layer using 400-mesh copper TEM grids. 2D Grazing-Incidence Wide-Angle X-ray Scattering (GIWAXS) measurements were carried out at the PLSII 9A U-SAXS beam line of Pohang Accelerator Laboratory, Korea.

2. Additional experimental results

The compatibility between two different materials can be evaluated by employing the equation:

$$\gamma_{A-B} = \gamma_A + \gamma_B - 4\left(\frac{\gamma_A^d \gamma_B^d}{\gamma_A^d + \gamma_B^d} + \frac{\gamma_A^p \gamma_B^p}{\gamma_A^p + \gamma_B^p}\right) \quad (5)$$

where $\gamma_{A\text{-}B}$ represents interfacial tension between material A and B. γ_A and γ_B are the surface tension of A and B, respectively. The superscript d and p represent the dispersion and polar components calculated using the contact angle with water and ethylene glycol (EG). The interfacial tension $\gamma_{BO\text{-}4Cl\text{-}Y7} \approx 0.09$ mN m^{-1} is much smaller than $\gamma_{B1\text{-}BO\text{-}4Cl} \approx 0.13$ mN m^{-1} and $\gamma_{B1\text{-}Y7} \approx 0.42$ mN m^{-1}, suggesting the good compatibility between BO-4Cl and Y7.

Table S1. Contact angle (CA), surface tension, Flory–Huggins interaction parameter (χ) and interfacial tension (γ) of the used materials,

X	Water CA [°]	EG CA [°]	γ^d [mN m^{-1}]	γ^p [mN m^{-1}]	Surface tension [mN m^{-1}]	$\chi_{BO\text{-}4Cl\text{-}X}$	$\chi_{Y7\text{-}X}$	$\gamma_{BO\text{-}4Cl\text{-}X}$ [mN m^{-1}]	$\gamma_{Y7\text{-}X}$ [mN m^{-1}]
B1	94.84	72.86	12.63	10.40	23.0	0.042	0.104	0.13	0.42
BO-4Cl	90.78	68.91	12.74	12.25	25.0	-	0.014	-	0.09
Y7	88.22	66.93	12.47	13.74	26.2	0.014	-	0.09	-

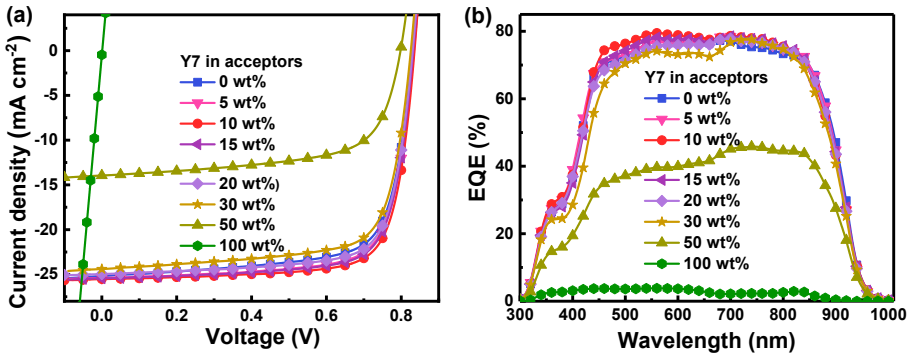

Figure S1. (a) *J-V* curves of ASM-OSCs with various Y7 content in acceptors under AM 1.5 G illumination at intensity of 100 mW cm^{-2}. (b) The EQE spectra of the corresponding ASM-OSCs.

The negligible power conversion efficiency (PCE) and open-circuit voltage (V_{OC}) of Y7-based binary cells (D/A=1/1) is probably related to the coarse morphology caused by the inferior solubility of Y7 and poor

compatibility between B1 and Y7. Y7 exhibit quite low solubility in chloroform, which is about 5 mg ml^{-1}. The photovoltaic properties of Y7-based binary cells with different D/A ratios were further studied, the concentration of donor is maintained as 10 mg ml^{-1}. The optimized Y7-based binary cells (D/A=1/0.3) achieve a PCE of 2.07% with a short-circuit current density (J_{SC}) of 9.71 mA cm^{-2}, a V_{OC} of 0.681 V and a fill factor (FF) of 31.22%.

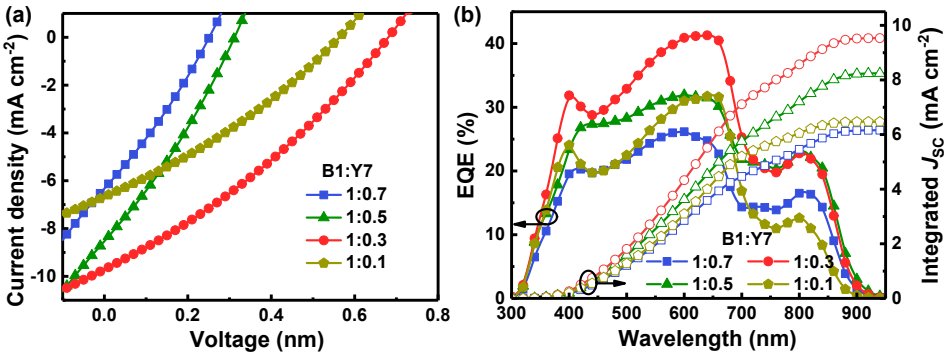

Figure S2. (a) *J-V* curves, (b) EQE spectra of Y7-based binary cells with different D/A ratios.

Table S2. Photovoltaic parameters of Y7-based binary cells with different D/A ratios

B1:Y7	J_{SC} [mA cm^{-2}]	Cal. J_{SC} [mA cm^{-2}]	V_{OC} [V]	FF [%]	PCE [%]
1:0.7	6.33	6.16	0.251	28.82	0.46
1:0.5	8.53	8.25	0.312	29.66	0.79
1:0.3	9.71	9.53	0.681	31.22	2.07
1:0.1	6.67	6.43	0.564	30.95	1.16

Table S3. Summary of the photovoltaic parameters for recent reported efficient ASM-OSCs.

System	J_{SC} [mA cm^{-2}]	FF [%]	V_{OC} [V]	PCE [%]	Reference
B1:BO-4Cl:Y7	25.52	76.29	0.836	16.28	In this work
ZnP-TSEH:6TIC:4TIC	25.95	75.57	0.81	15.88	[7]
BTR-Cl:Y6:$PC_{71}BM$	23.75	77.11	0.84	15.34	[8]
B1:BO-4Cl	25.27	73	0.83	15.3	[9]
TBD-S4:Y6	24.53	72.1	0.854	15.1	[10]
ZR2-C3:Y6	24.69	70.06	0.854	14.78	[11]
BTR-Cl:Y6	23.83	74.7	0.83	14.7	[12]
ZR1:Y6	24.34	68.44	0.861	14.34	[13]
BT-2F:N3	23.81	70.22	0.84	14.09	[14]
SM1-F:Y6	23.25	69.9	0.866	14.07	[15]
BTTZR:Y6	23.2	68	0.88	13.9	[16]
BSFTR:Y6	23.16	69.66	0.85	13.69	[17]
BTR:NITI:$PC_{71}BM$	19.5	73.83	0.94	13.63	[18]
BTR-Cl:Y6	24.17	65.5	0.86	13.61	[19]
BTEC-2F:Y6	21.55	72.35	0.85	13.34	[20]

The absorption spectra of active layers (R_1-R_2) were calculated by subtracting the parasitic absorptions (1-R_1) from the total absorption in ASM-OSCs (1-R_2), where R_1 is the reflection spectrum of the standard sample of the equipment, R_2 is the reflection spectra of ASM-OSCs with structure of ITO/PEDOT:PSS/active layers/PNDIT-F3N/Al. The internal quantum efficiency (IQE) spectra can be obtained according to the equation of EQE/(R_1-R_2). The intact absorption spectra of active layer in the typical ASM-OSCs and corresponding IQE spectra is shown in **Figure S3**.

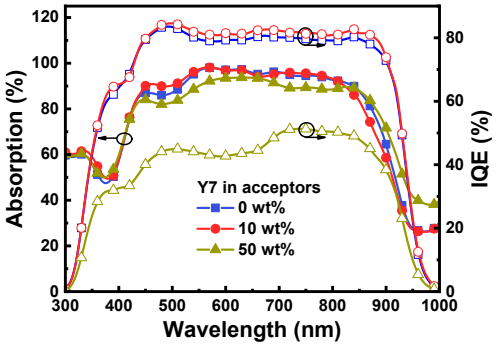

Figure S3. Absorption spectra of active layer in the typical ASM-OSCs and the corresponding IQE spectra.

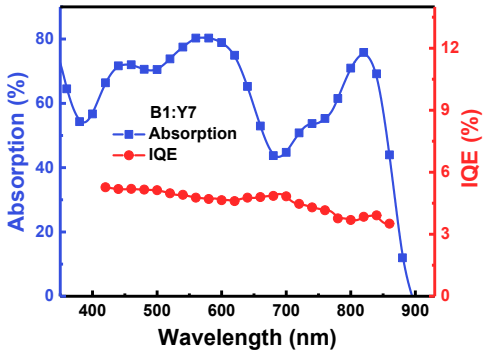

Figure S4. Absorption spectra of active layer in Y7-based binary cells (D/A=1:1) and the corresponding IQE spectra.

Table S4. Key parameters of the typical ASM-OSCs

Y7 in acceptors [wt%]	J_{sat} **[mA cm^{-2}]**	J_{ph}* **[mA cm^{-2}]**	$J_{ph}^{\&}$ **[mA cm^{-2}]**	J_{ph}*/J_{sat} (η_g) **[%]**	$J_{ph}^{\&}$/J_{sat} (η_e) **[%]**
0	26.55	25.18	22.18	94.84	83.54
10	26.61	25.52	23.23	95.90	87.30
50	17.02	13.95	11.09	81.96	65.16

J_{sat}: The J_{ph} under condition of V_{eff}=3 V

J_{ph}*: The J_{ph} under short circuit conditions

$J_{ph}^{\&}$: The J_{ph} under maximum power output conditions

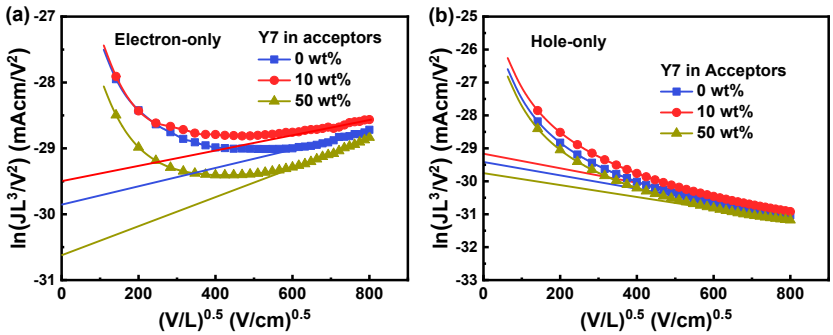

Figure S5. The $\ln(JL^3/V^2)$ vs $(V/L)^{0.5}$ curves of (a) electron-only ITO/ZnO/active layer/PNDIT-F3N/Al devices and (b) hole-only ITO/PEDOT:PSS/active layer/MoO_3/Ag devices.

Table S5. The electron mobility (μ_e), hole mobility (μ_h) values of the active layers with various Y7 content.

Y7 in acceptors [wt%]	μ_e [$cm^2\ V^{-1}\ s^{-1}$] Max (Avg.±Dev.[a)])	μ_h [$cm^2\ V^{-1}\ s^{-1}$] Max (Avg.±Dev.[a)])
0	$3.60\ (3.21\pm0.41)\times10^{-4}$	$5.76\ (5.48\pm0.30)\times10^{-4}$
10	$5.16\ (4.85\pm0.33)\times10^{-4}$	$7.11\ (6.95\pm0.26)\times10^{-4}$
50	$1.66\ (1.14\pm0.54)\times10^{-4}$	$4.02\ (3.57\pm0.46)\times10^{-4}$

[a)]Average (Avg.) mobility values and the deviations (Dev.) based on individual 10 cells

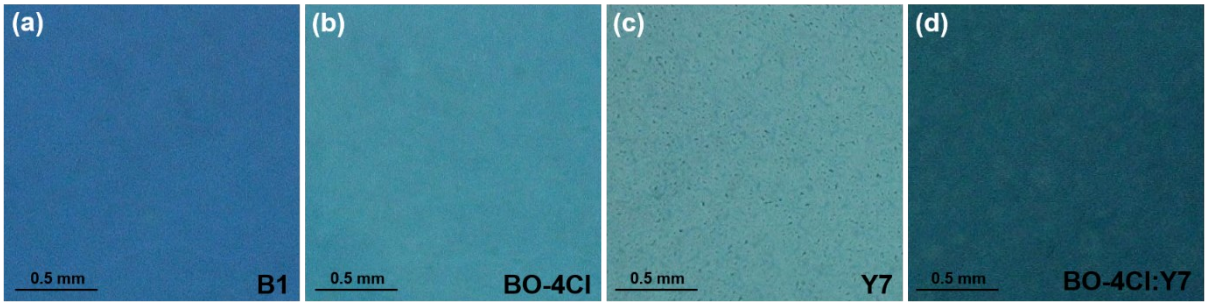

Figure S6. OM images of pure films and BO-4Cl:Y7 (1:1) blend films, the pure films are prepared based on the solution with concentration of 10 mg ml^{-1} and the blend films are fabricated with 20 mg ml^{-1} solution.

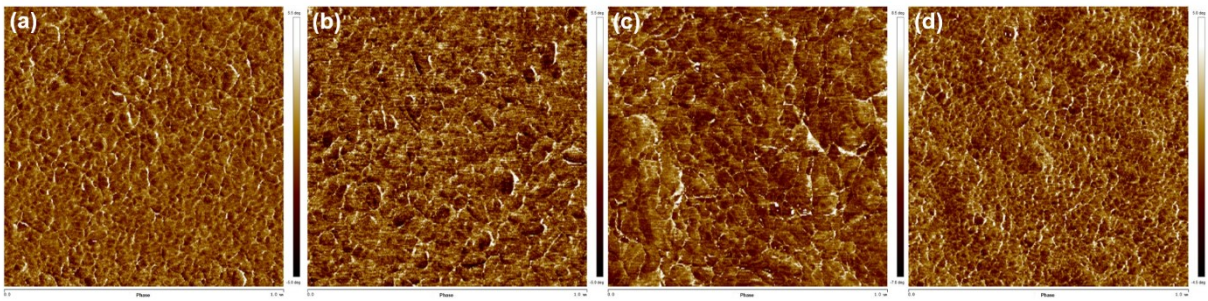

Figure S7. AFM phase images of blend films with (a) 0 wt%, (b) 10 wt%, (c) 50 wt% and (d) 100 wt% Y7 in acceptors.

Table S6. Crystallographic parameters of neat and blend films for the used materials. OOP: out-of-plane. IP: in-plane. CCL: crystal coherence length.

Component	IP				OOP			
	100		010		100		010	
	d-spacing (Å)	CCL (nm)	d-spacing (Å)	CCL (nm)	d-spacing (Å)	CCL (nm)	d-pacing (Å)	CCL (nm)
B1	-	-	3.65	7.85	20.26	19.4	-	-
BO-4Cl	16.10	5.10	-	-	-	-	3.67	2.18
Y7	14.60	9.72	-	-	-	-	3.67	2.49
B1:BO-4Cl	20.93	6.90	-	-	15.67	-	3.76	2.88
10 wt% Y7	20.26	13.36	-	-	-	-	3.70	4.25
50 wt% Y7	20.26	9.37	-	-	-	-	3.70	3.79
B1:Y7	20.26	7.21	3.62	-	-	-	3.69	3.29

Reference

1. H. Cha, D. S. Chung, S. Y. Bae, M. J. Lee, T. K. An, J. Hwang, K. H. Kim, Y. H. Kim, D. H. Choi, C. E. Park, *Adv. Funct. Mater.* 2013, **23**, 1556.

2. S. Y. Chang, H. C. Liao, Y. T. Shao, Y. M. Sung, S. H. Hsu, C. C. Ho, W. F. Su, Y. F. Chen, *J. Mater. Chem. A*. 2013, **1**, 2447.

3. Y. Zhang, D. Deng, K. Lu, J. Zhang, B. Xia, Y. Zhao, J. Fang, Z. Wei, *Adv. Mater.* **2015**, 27, 1071.

4. Z. S. An, J. S. Yu, S. C. Jones, S. Barlow, S. Yoo, B. Domercq, P. Prins, L. D. A. Siebbeles, B. Kippelen, S. R. Marder, *Adv. Mater*. 2005, **17**, 2580.

5. M. Koppe, H. J. Egelhaaf, G. Dennler, M. C. Scharber, C. J. Brabec, P. Schilinsky, C. N. Hoth, *Adv. Funct. Mater.* 2010, **20**, 338.

6. Y. X. Chen, X. Zhang, C. L. Zhan, J. N. Yao, *ACS Appl. Mater. Interfaces*. 2015, **7**, 6462.

7. L. Nian, Y. Kan, K. Gao, M. Zhang, N. Li, G. Zhou, S. B. Jo, X. Shi, F. Lin, Q. Rong, *Joule* 2020, **4**, 2223.

8. D. Hu, Q. Yang, H. Chen, F. Wobben, V. M. Le Corre, R. Singh, T. Liu, R. Ma, H. Tang, L. J. A. Koster, *Energy Environ. Sci*. 2020. **13**, 2134.

9. J. Qin, C. An, J. Zhang, K. Ma, Y. Yang, T. Zhang, S. Li, K. Xian, Y. Cui, Y. Tang, *Sci. China Mater.* 2020, **63**, 1142.

10. X. Wang, J. Wang, J. Han, D. Huang, P. Wang, L. Zhou, C. Yang, X. Bao, R. Yang, *Nano Energy* 2020, DOI: 10.1016/j.nanoen.2020.105612.

11. R. Zhou, Z. Jiang, Y. Shi, Q. Wu, C. Yang, J. Zhang, K. Lu, Z. Wei, *Adv. Funct. Mater.* 2020, **30**, 2005426.

12. H. Tang, H. Y. Chen, C. Q. Yan, J. M. Huang, P. W. K. Fong, J. Lv, D. Q. Hu, R. Singh, M. Kumar, Z. Y. Xiao, Z. P. Kan, S. R. Lu, G. Li, *Adv. Energy Mater*. 2020, **10**, 2001076.

13. R. M. Zhou, Z. Y. Jiang, C. Yang, J. W. Yu, J. R. Feng, M. A. Adil, D. Deng, W. J. Zou, J. Q. Zhang, K. Lu, W. Ma, F. Gao, Z. X. Wei, *Nat. Commun.* 2019, **10**, 5393.

14. J. Gao, J. Ge, R. Peng, C. Liu, L. Cao, D. Zhang, B. Fanady, L. Hong, E. Zhou, Z. Ge, *J. Mater. Chem. A* 2020, **8**, 7405.

15. B. B. Qiu, Z. Chen, S. C. Qin, J. Yao, W. C. Huang, L. Meng, H. M. Zhu, Y. Yang, Z. G. Zhang, Y. F. Li, *Adv. Mater.* 2020, **32**, 1908373.

16. Y. L. Wang, Y. Wang, L. Zhu, H. Q. Liu, J. Fang, X. Guo, F. Liu, Z. Tang, M. J. Zhang, Y. F. Li, *Energy Environ. Sci.* 2020, **13**, 1309.

17. Q. Yue, H. Wu, Z. Zhou, M. Zhang, F. Liu, X. Zhu, *Adv. Mater.* 2019, **31**, 1904283.

18. Z. Zhou, S. Xu, J. Song, Y. Jin, Q. Yue, Y. Qian, F. Liu, F. Zhang, X. Zhu, *Nat. Energy* 2018, **3**, 952.

19. H. Y. Chen, D. Q. Hu, Q. G. Yang, J. Gao, J. H. Fu, K. Yang, H. He, S. S. Chen, Z. P. Kan, T. N. Duan, C. Yang, J. Y. Ouyang, Z. Y. Xiao, K. Sun, S. R. Lu, *Joule* 2019, **3**, 3034.

20. J. Ge, L. Xie, R. Peng, B. Fanady, J. Huang, W. Song, T. Yan, W. Zhang, Z. Ge, *Angew. Chem. Int. Ed.* 2020, **59**, 2808.